CORROSION SCIENCE AND TECHNOLOGY, Vol.21, No.5(2022), pp.327~339 pISSN 1598-6462 / eISSN 2288-6524
[Research Paper] DOI: https://doi.org/10.14773/cst.2022.21.5.327

Effect of Water Impingement Conditions on the Degradation of Epoxy Coatings in Tap Water

D. H. Kim, Y. R. Yoo, and Y. S. Kim†

Materials Research Centre for Energy and Clean Technology, School of Materials Science and Engineering, Andong National University, 1375 Gyeongdong-ro, Andong, Gyeongbuk, 36729, Korea
(Received October 07, 2022; Revised October 20, 2022; Accepted October 21, 2022)

The water-jet technique started by Bridgman can cut metal and alloys without harmful gas and fume. However, while this technique is convenient to cut metals and alloys, in the case of coated pipe, water jet induces the degradation of coatings on the pipes, and may facilitate structural failure, leakage, and loss of products. While there are many reports on the effect of water jet on cut metals and the damage of metallic materials, research on the effect of water impingement on the epoxy coatings has been little studied. In this work, we therefore control the velocity of water jet, distance between nozzle and specimen, and water temperature, and discuss the effect of water impingement on the epoxy coatings. Increasing water velocity and water temperature and reducing nozzle distance increased the degradation rates of three epoxy coatings were increased. Among three test parameters – water velocity, nozzle distance and water temperature, water temperature was relatively effective to increase the degradation rate of epoxy coatings.

Keywords: *Epoxy coating, Water impingement, Velocity, Nozzle distance, Temperature*

1. Introduction

Many facilities in power plants, ships, marine plants, and the like used seawater as cooling water. Although seawater is very useful in many fields, it may induce the corrosion of metals and alloys. In particular, it is well known that carbon steel and low-alloy steels experience severe corrosion problems [1-4]. Chloride ion in seawater is one of the very aggressive ions to attack metal and alloys, and increases in dissolved oxygen and temperature stimulated the internal corrosion of pipings [5-7]. In addition, because of the use of seawater as cooling water, scale on the heat exchanger can be formed by chloride, etc., and thus there are much leakage from piping by corrosion [8].

To solve the corrosion and leaks problem, internally coated pipes have been used [9-11]. When coatings are applied, they can prevent the contact of pipe with seawater, thus protect the pipe from corrosion and increase its lifespan, and therefore reduce the cost of maintenance [12]. Among interior coated piping, rubber-lined and epoxy-coated piping have been extensively used in many industrial fields. Rubber lining offers good performance to corrosion, heat, and wear, while epoxy coating shows good adherence and formability, and high chemical and corrosion resistance [13]. Epoxy materials have been extensively used to protect the structure for several reasons [14-16]. However, these kinds of coatings may suffer damage because of cavitation, water impingement, and variation of temperature and pressure in long-term operation [17-20]. There are many reports of the damage of rubber-lined or epoxy-coated pipes, even after a short period of use [21-23]. Cavitation damage can occur in areas showing high variation of velocity and pressure of fluid used in hydraulic turbine, elbow of pipe, propeller in ships, pump impeller, etc. [24]. Fluctuation in pressure results in the formation and collapse of vapor, exerts repetitive impact near the surface, and finally induces cavitation degradation [25]. Fluid collision with the surface is important in many fields, and may induce severe erosion, as shown in the steam turbine [26]. When cavitation properties by solution temperature were tested for the three kinds of epoxy coatings, in addition to the cushioning effect, the reason that the cavitation degradation rate reduced with solution temperature was partly related to the brittle fracture and

†Corresponding author: yikim@anu.ac.kr
D. H. Kim: Master course, Y. R. Yoo: Ph.D., Senior researcher, Y. S. Kim: Professor

Table 1. Chemical composition of the experimental epoxy coatings

Coating	wt.%	C	O	Si	Ti	Na	Mg	Al	K	Ca	Zn
A	Matrix	26.6	72.02	0.52	0.86	-	-	-	-	-	-
	Compound	-	46.51	33.22	-	7.84	1.48	2.41	0.86	4.89	2.79
B	Matrix	26.51	72.03	0.91	0.55	-	-	-	-	-	-
	Compound	-	45.41	33.11	-	6.59	1.58	2.99	1.88	5.72	2.72
C	Matrix	26.78	72.26	0.57	0.39	-	-	-	-	-	-
	Compound	5.11	56.9	37.99	-	-	-	-	-	-	-

water absorptivity of the epoxy coatings, and the water density, but was little related to the shape and composition of the compound in the coatings, or the phase transition of the epoxy coating [20].

Research on the water-jet effect started by Bridgman has been conducted, and this technique can cut metal and alloys without harmful gas and fume [27]. While this technique is convenient to cut metals and alloys, in the case of coated pipe, water jet induces the degradation of coatings on the pipes, and may facilitate structural failure, leakage, loss of products, etc. [28]. Although there are many reports on the effect of water jet on the cut metals and the damage of metallic materials, little research has been conducted on the effect of water impingement on the epoxy coatings.

In this work, therefore, we control the velocity of water jet, the distance between nozzle and specimen, and water temperature, and discuss the effect of water impingement on the epoxy coatings.

2. Experimental Methods

2.1 Materials

Three kinds of epoxy coating were used, with specimen made by each manufacturer, and named ‘A coating’, ‘B coating’, and ‘C coating’. The specimen was disc type, and of 32 mm diameter. Table 1 shows the chemical composition of the specimen, which was analyzed by EDS (Energy Dispersive Spectroscope, Tescan, Brno, Czech Republic).

2.2 Water Impingement Test

Fig. 1 shows a schematic of the water impingement tester (Jet Erosion Tester, R&B, Korea) that was fabricated according to ISO 16925 standard [29]. The test solution was tap water, and the test temperature was

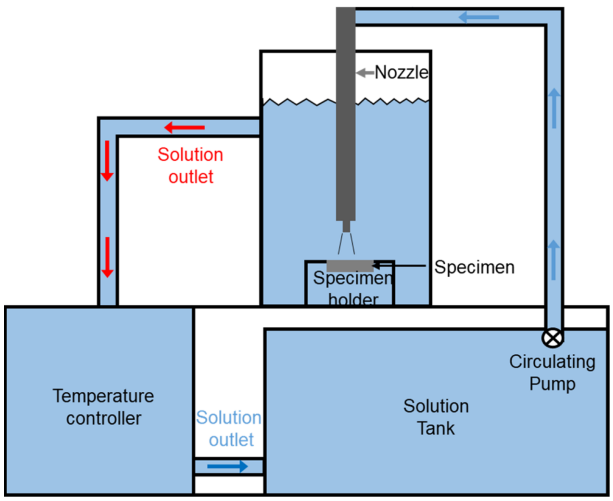

Fig. 1. Schematic of the water impingement tester

(15, 30, & 45) ºC. We controlled the water velocity (water pressure) as (80, 113, & 139) m/s at (2, 4, & 6) MPa, and varied the distance between the specimen and the nozzle as (10, 30, & 60) mm. Tests were performed for (30, 60, & 90) min at each condition, and its degradation rate was calculated by weight loss.

2.3 Surface Analysis

Surface appearance was analyzed using a digital camera and SEM (MIRA3XMH, Tescan, Brno, Czech Republic). Chemical composition was measured using EDS. The surface of the specimen was coated using osmium and the center area and the boundary of the water-impinged area were analyzed.

3. Results and Discussion

3.1 Surface appearance and components of the specimen

Fig. 2 shows the surface appearance by digital camera

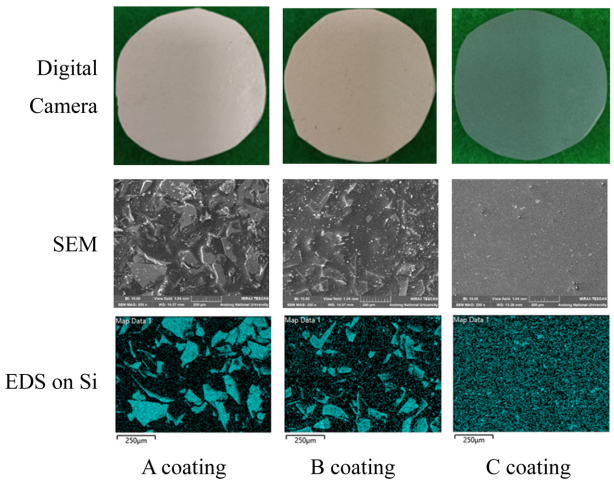

Fig. 2. Surface appearance, SEM image, and EDS on Si of the epoxy coatings before test

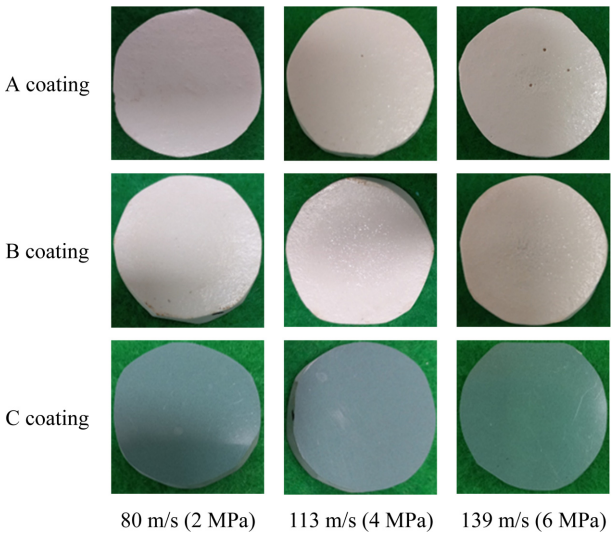

Fig. 3. Effect of water impingement velocity on the surface appearance of epoxy coatings using a tap water at 30 °C and a nozzle distance of 30 mm

and SEM image of the surface and Si distribution by EDS of the three epoxy coatings before test. The shape of strengthening materials of A and B coatings is plate-like, while the shape of C coating is granule-type. The A coating consists of glass flake of (3 ~ 4) μm thickness and (0.4 ~ 3.2) mm width in polyester epoxy resin as a high-performance thermoset vinyl ester; A coating shows good performance to wear and erosion, and thus this coating has been used for erosion-resistant and corrosion protection. The B coating consists of acrylic glass flake in iso-phthalic polyester, and its maximum temperature is restricted to under 60 °C. On the other hand, the C coating consists of ceramic compound in an epoxy resin [30].

3.2 Effect of water impingement velocity on the degradation of epoxy coatings

Fig. 3 shows the effect of water impingement velocity on the surface appearance of epoxy coatings using tap water at 30 ºC. The distance between the nozzle and the specimen was 30 mm. The approximate water impinged area was of 11 mm diameter. The water impingement velocity was controlled as (80, 113, & 139) m/s at (2, 4, & 6) MPa, respectively, and the test time was 90 min. In the case of A and B coatings, increased water pressure induced the degradation of the surface, and revealed some pores in the coatings. On the other hand, little degradation of the surface appearance of C coating was observed on a digital photograph.

Fig. 4 shows the effect of water impingement time and velocity on the degradation of epoxy coatings using tap water at 30 °C, as described in Fig. 3. Fig. 4a, b, & c show the effect of test time under (80, 113, & 139) m/s at (2, 4, & 6) MPa, respectively, on the degradation rate. At low velocity, the rates were similar to each other, but with increasing water velocities, the rates of the three coatings show different resistance. Fig. 4d shows the degradation rate after test for 90 min, and regardless of water velocities, the rate of C coating was the lowest among the three epoxy coatings.

Fig. 5 shows the surface appearance of A coating after water impingement test for 90 min using tap water at 30 ºC, and a nozzle distance of 30 mm. Fig. 5a shows the center area, while Fig. 5b shows the boundary area by water impingement. At low velocity, the surface appearance was similar to that of the specimen before test, as shown in Fig. 2, but increasing the water velocities, glass flakes, including epoxy resin, were detached and new internal components were revealed. Fig. 6 shows the EDS result on Si of A coating (the specimen was the same in Fig. 5) after water impingement test for 90 min using tap water at 30 ºC, and a nozzle distance of 30 mm. Glass flake of the center area including the boundary area was detached even at low water velocity. At high water velocity, the distribution of the glass flake was similar to that of the

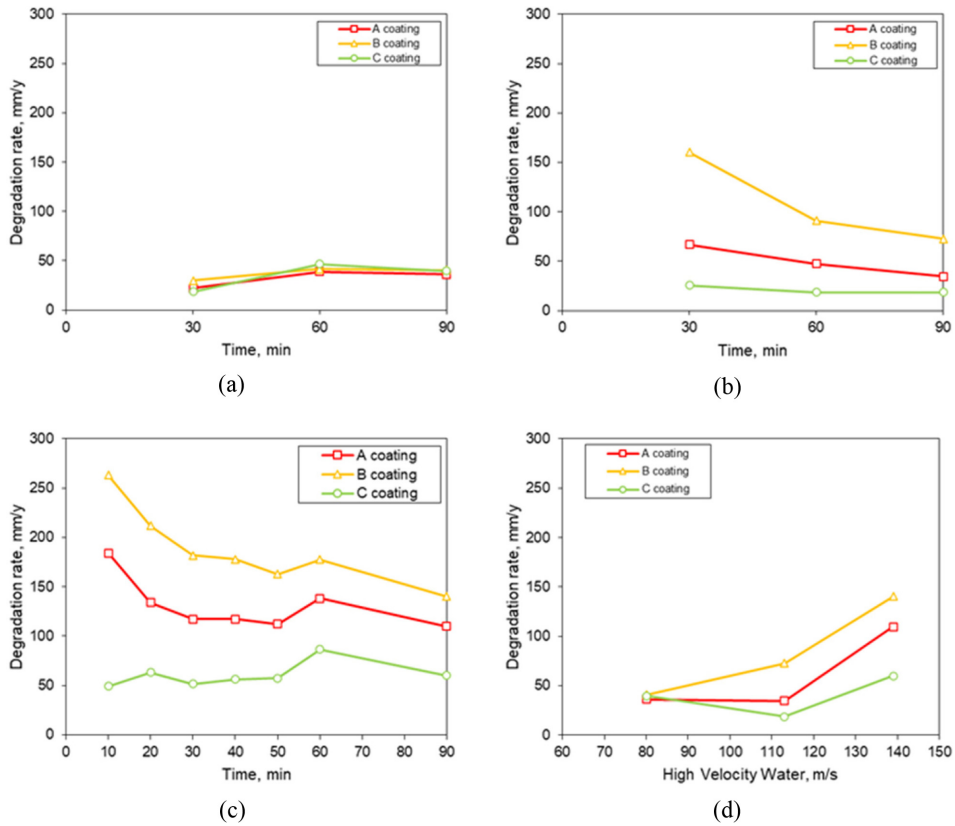

Fig. 4. Effect of water impingement time and velocity on the degradation of epoxy coatings using a tap water at 30 °C and a nozzle distance of 30 mm; (a) 80 m/s at 2 MPa, (b) 113 m/s at 4 MPa, (c) 139 m/s at 6 MPa, and (d) degradation rate after test

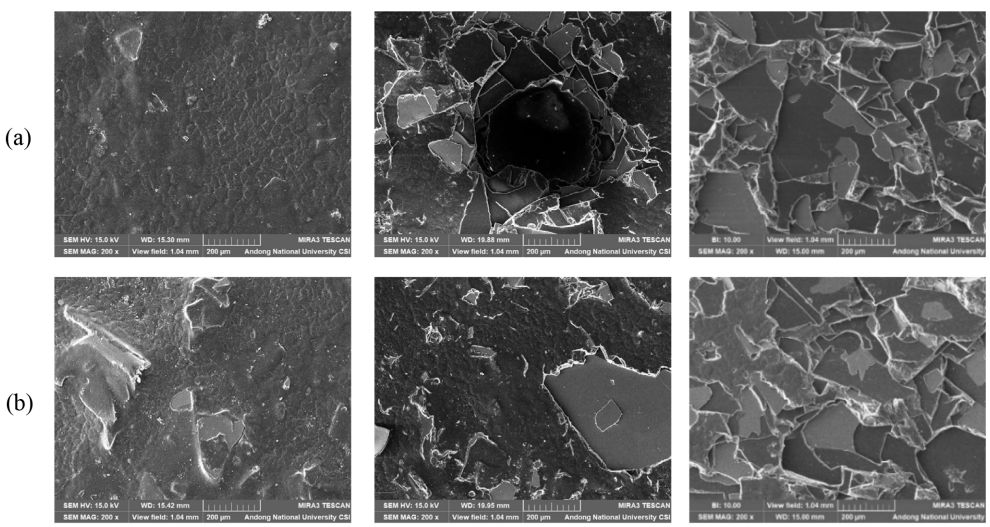

Fig. 5. Surface appearance of A coating after water impingement test for 90 min using tap water at 30 °C, and a nozzle distance of 30 mm: (a) Center area, and (b) Boundary area

specimen before test, as shown in Fig. 2.

Fig. 7 shows the surface appearance of B coating after water impingement test for 90 min using tap water at 30 °C, and a nozzle distance of 30 mm. Fig. 7a shows the center area, while Fig. 7b shows the boundary area by water impingement. The surface appearance was

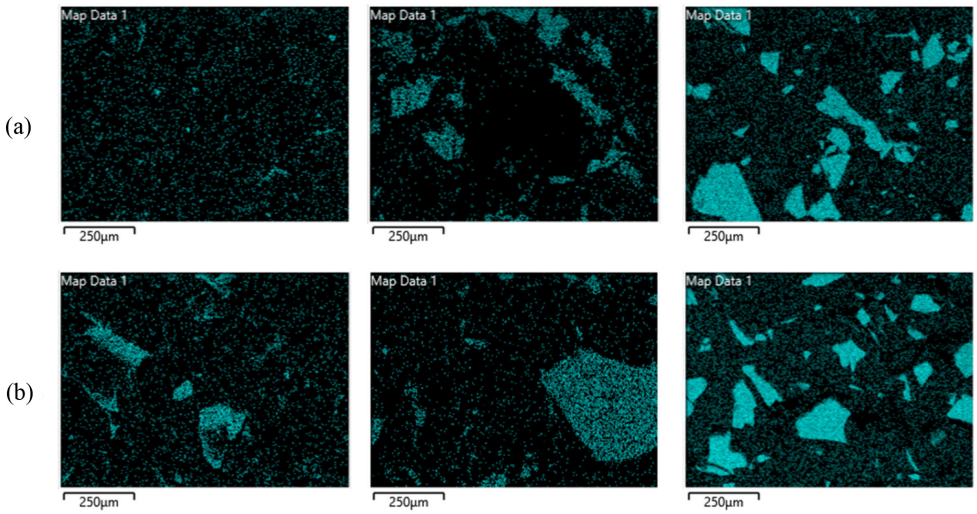

Fig. 6. EDS result on Si of A coating after water impingement test for 90 min using tap water at 30 °C, and a nozzle distance of 30 mm: (a) Center area, and (b) Boundary area

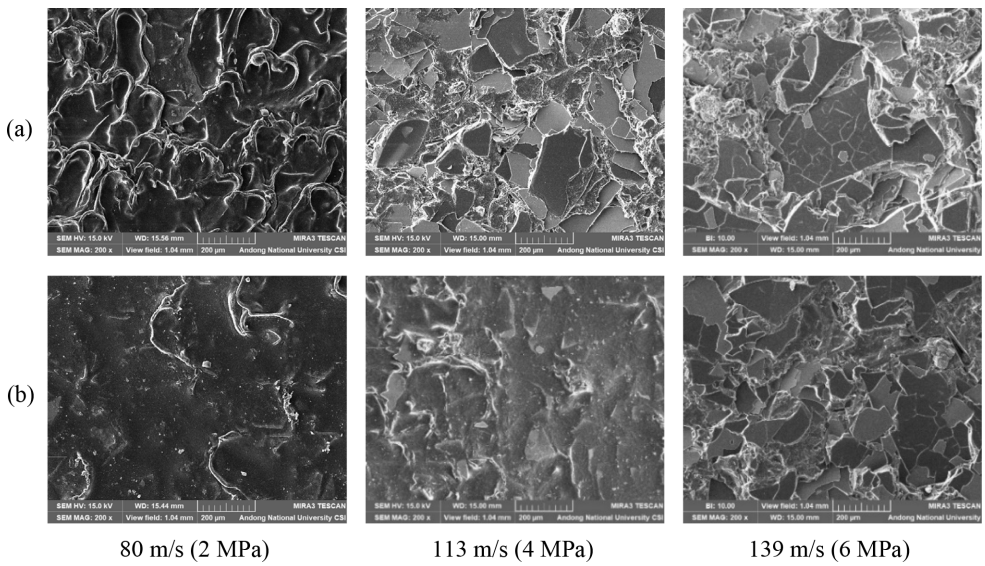

Fig. 7. Surface appearance of B coating after water impingement test for 90 min using tap water at 30 °C, and a nozzle distance of 30 mm: (a) Center area, and (b) Boundary area

damaged even at low water velocity, and on increasing the water velocities, glass flakes, including epoxy resin, were detached, and the interior components were revealed. Fig. 8 shows the EDS result on Si of B coating (the specimen was the same in Fig. 7) after water impingement test for 90 min using tap water at 30 °C, and a nozzle distance of 30 mm. Glass flake of the center area, including the boundary area, was detached, even at low water velocity. At high water velocity, the distribution of the glass flake was similar to that of the specimen before test, as shown in Fig. 2.

Fig. 9 shows the surface appearance of C coating after water impingement test for 90 min using tap water at 30 °C, and a nozzle distance of 30 mm. Fig. 9a shows the center area, while Fig. 9b shows the boundary area by water impingement. The surface appearance was little changed even at high water velocity, except for newly emerging pore on the center area. Fig. 10 shows the

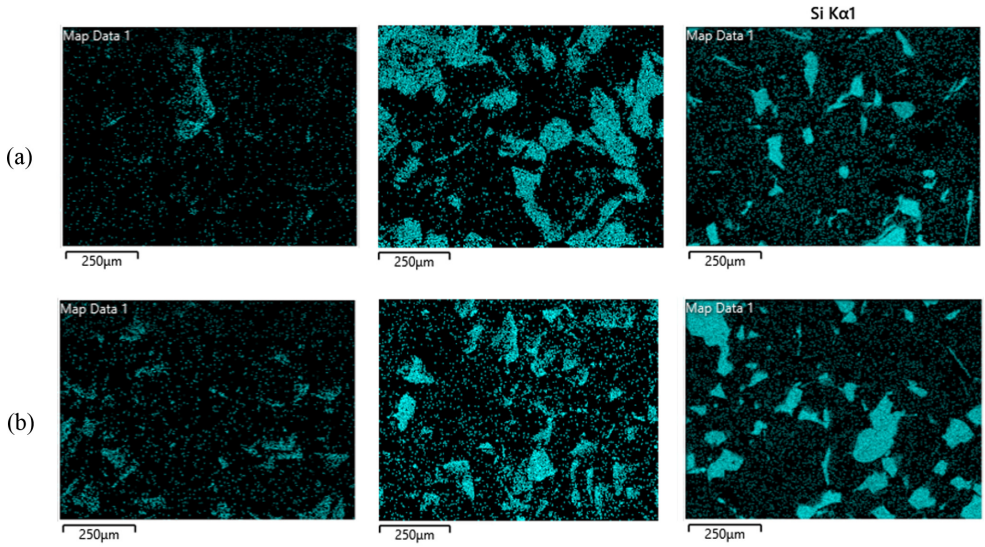

Fig. 8. EDS result on Si of B coating after water impingement test for 90 min using tap water at 30 °C, and a nozzle distance of 30 mm: (a) Center area, and (b) Boundary area

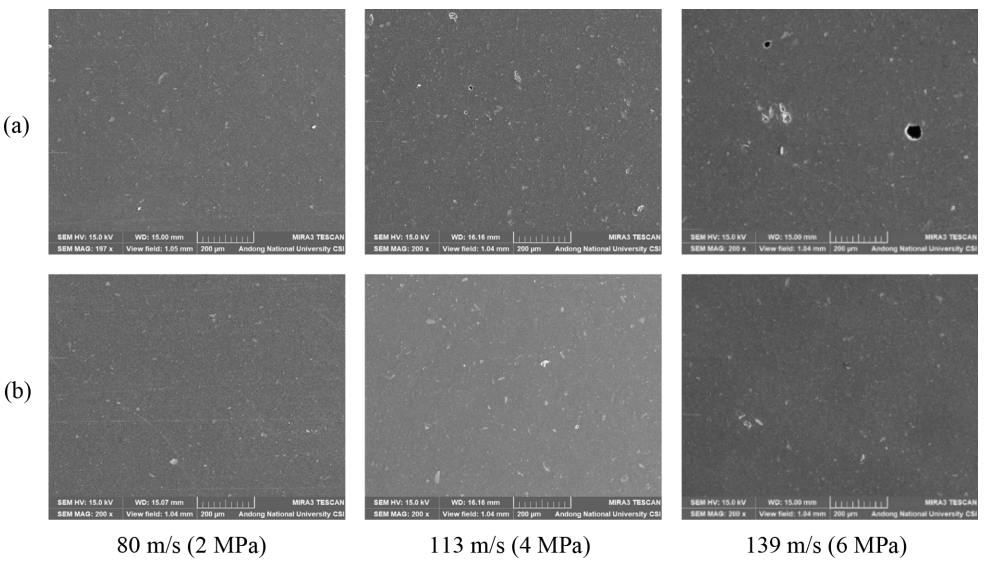

Fig. 9. Surface appearance of C coating after water impingement test for 90 min using tap water at 30 °C, and a nozzle distance of 30 mm: (a) Center area, and (b) Boundary area

EDS result on Si of C coating (the specimen was the same in Fig. 9) after water impingement test for 90 min using tap water at 30 °C, and a nozzle distance of 30 mm. The distribution of ceramic compounds was the same, regardless of water velocity.

3.3 Effect of the distance between nozzle and specimen on the degradation of epoxy coatings

Fig. 11 shows the effect of nozzle distance on the surface appearance of epoxy coatings after water impingement test for 90 min using tap water at 30 °C and water velocity of 139 m/s. The diameter of the water-impinged area was approximately (6, 11, & 15) mm at a nozzle distance of (10, 30, & 60) mm, respectively. In the case of A coating, when the nozzle distance decreased, the pores emerged, and the damage depth increased. In the case of B coating, similar damage was observed to the A coating. However, little damage was

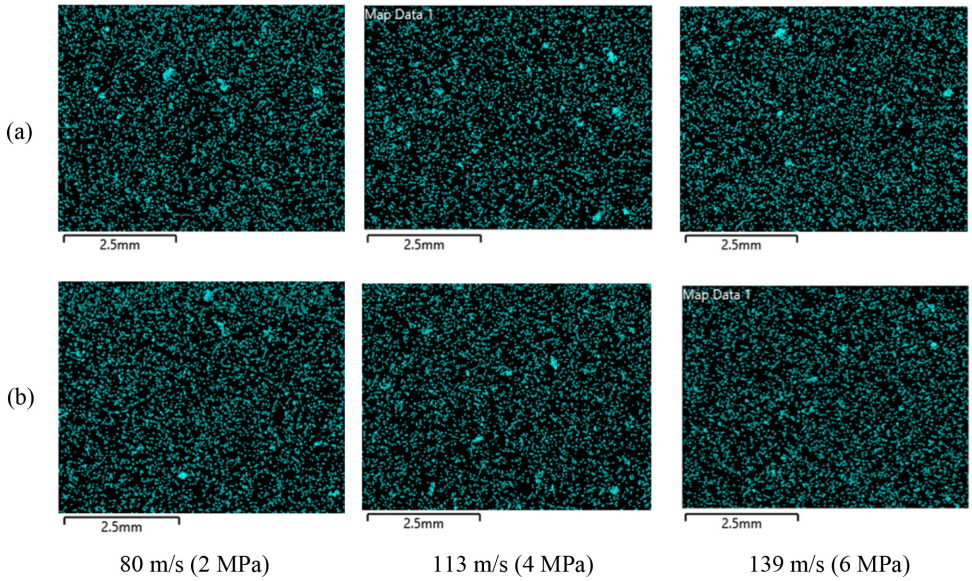

Fig. 10. EDS result on Si of C coating after water impingement test for 90 min using tap water at 30 °C, and a nozzle distance of 30 mm: (a) Center area, and (b) Boundary area

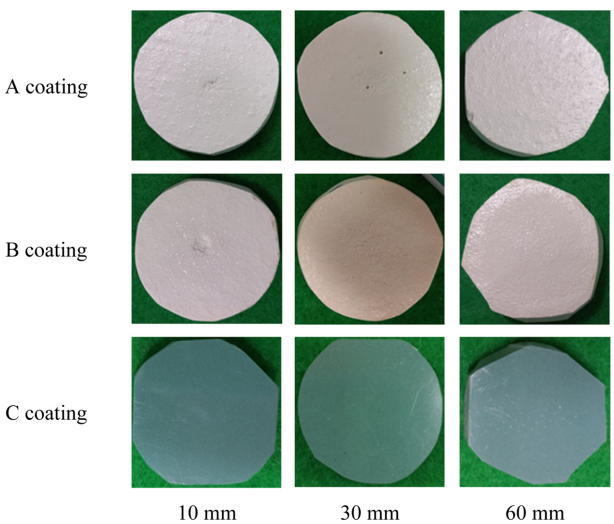

Fig. 11. Effect of nozzle distance on the surface appearance of epoxy coatings after water impingement test for 90 min using tap water at 30 °C and water velocity of 139 m/s

observed at the close nozzle distance in the case of C coating.

Fig. 12 shows the effect of test time and water impingement distance between the nozzle and specimen on the degradation rate using tap water at 30 ºC and water velocity of 139 m/s. At the nozzle distance of 10 mm, the difference of degradation rate was larger than those of other nozzle distances, but increasing the nozzle distance, the difference was reduced. Fig. 12d shows the effect of the nozzle distance on the rate after 90 min test; among the three epoxy coatings, C coating showed higher resistance to the water impingement environment.

Fig. 13 shows the effect of nozzle distance on SEM images (center area) after water impingement test for 90 min using tap water at 30 ºC and water velocity of 139 m/s. In the case of A and B coatings, big holes were formed at the nozzle distance of 10 mm. However, small pore was observed in C coating. Fig. 14 shows the effect of nozzle distance on Si strengthener by EDS (center area) after water impingement test for 90 min using tap water at 30 ºC and water velocity of 139 m/s. In the cases of A and B coatings, the glass flakes were detached, and the Si distribution was non-uniform. However, in the case of C coating, the Si distribution was similar to that of the specimen before test, as shown in Fig. 2.

3.4 Effect of impingement water temperature on the degradation of epoxy coatings

Fig. 15 shows the effect of water temperature on the surface appearance of epoxy coatings after water impingement test for 90 min using tap water at a nozzle distance of 10 mm and water velocity of 139 m/s. In the case of A and B coatings, the increased water temperature deeply impacted the surface appearance, and the coatings were greatly detached. In particular, its impact was highest at 45 ºC. However, in the case of C

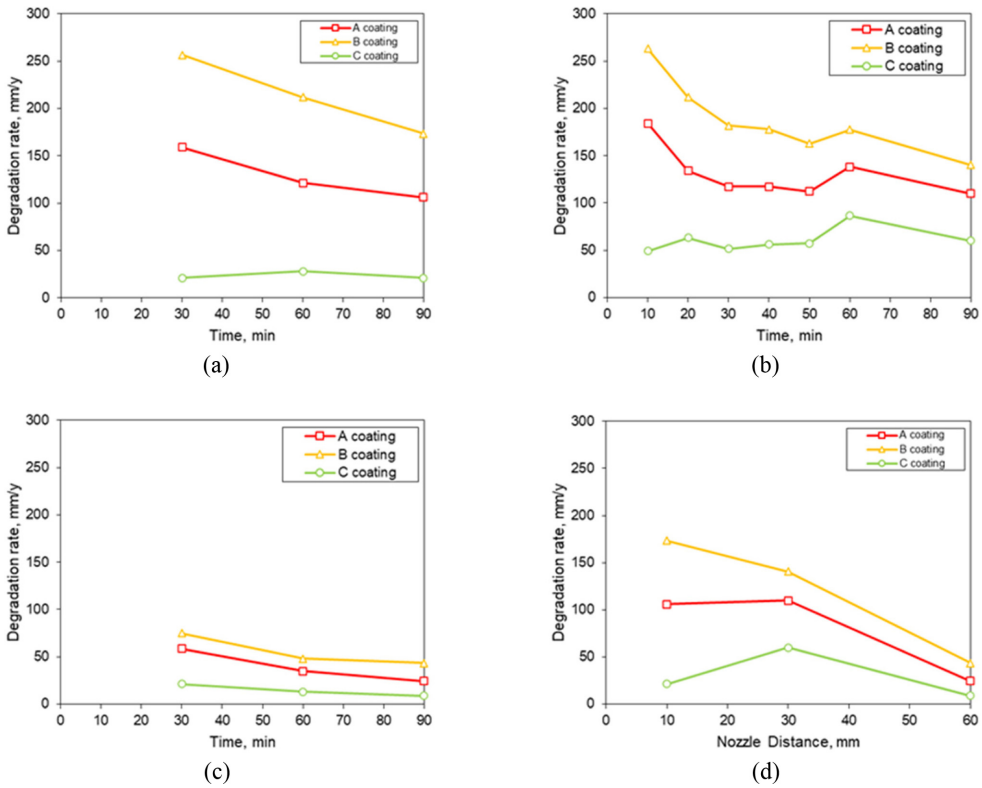

Fig. 12. Effect of test time and water impingement distance between the nozzle and the specimen on the degradation rate using tap water at 30 °C and water velocity of 139 m/s: (a) 10 mm (b) 30 mm (c) 60 mm, and (d) degradation rate after test

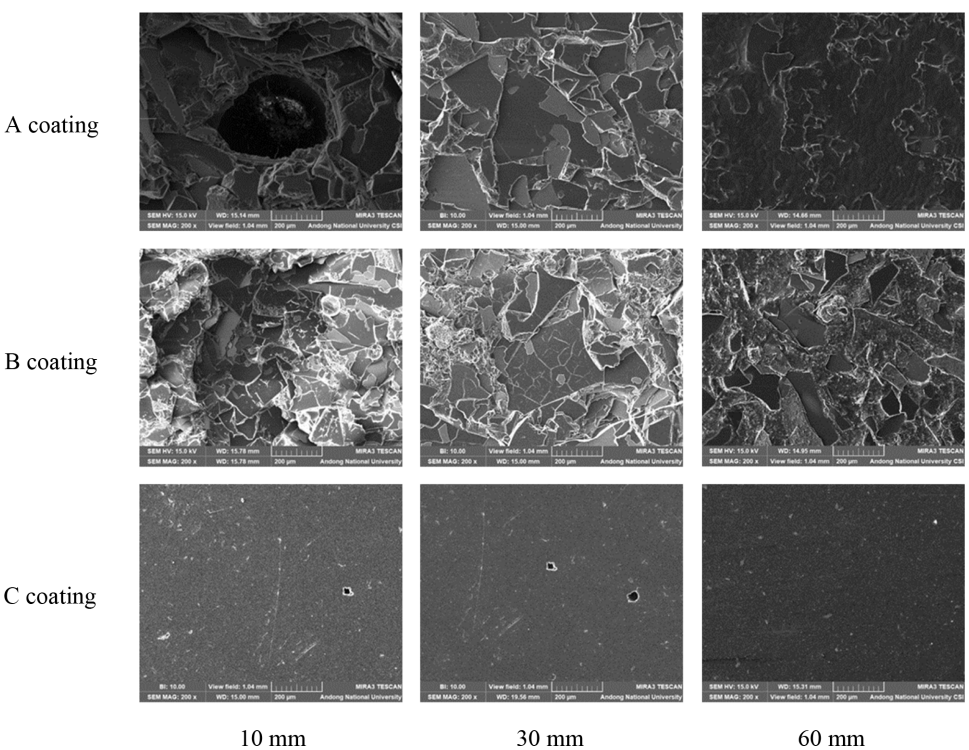

Fig. 13. Effect of nozzle distance on SEM images (center area) after water impingement test for 90 min using tap water at 30 °C and water velocity of 139 m/s

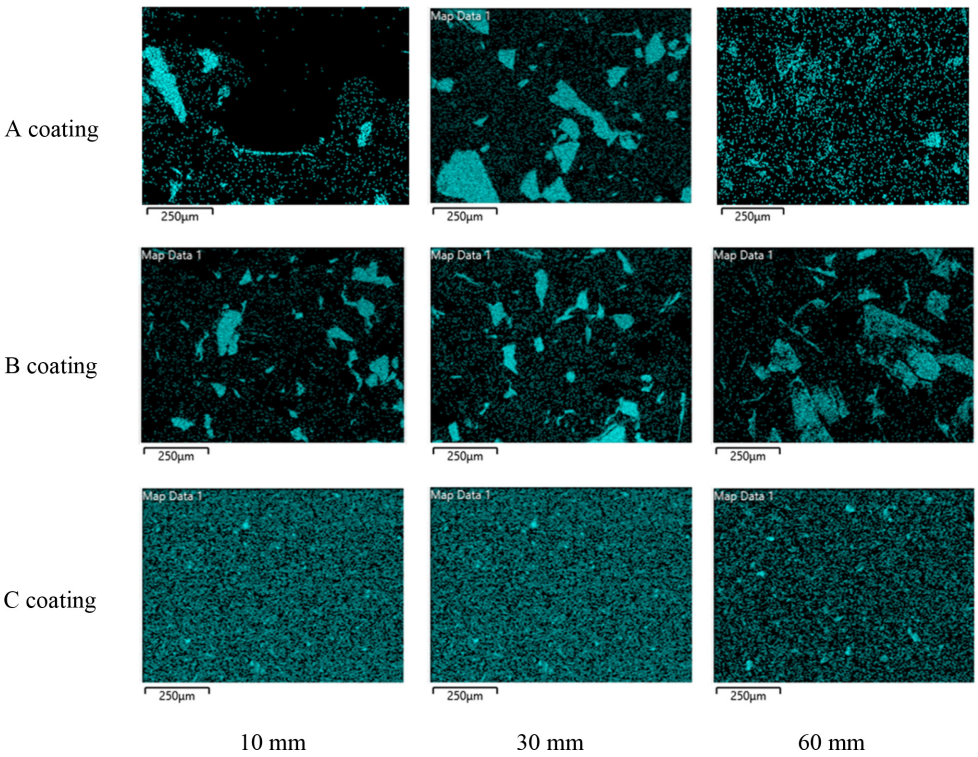

Fig. 14. Effect of nozzle distance on Si strengthener by EDS (center area) after water impingement test for 90 min using tap water at 30 °C and water velocity of 139 m/s

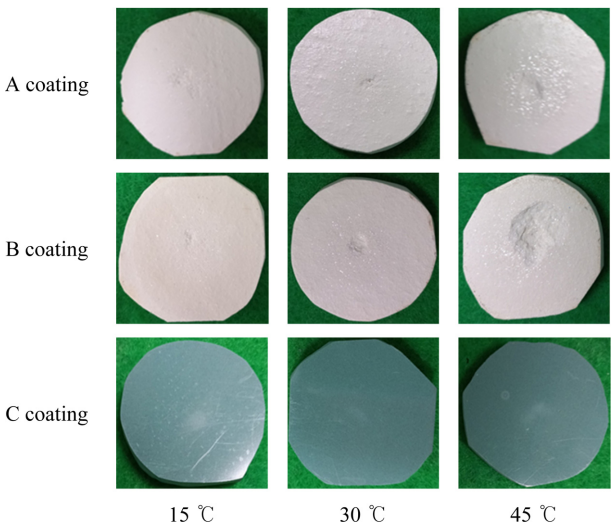

Fig. 15. Effect of water temperature on the surface appearance of epoxy coatings after water impingement test for 90 min using tap water at a nozzle distance of 10 mm and water velocity of 139 m/s

coating, the surface appearance was little affected by the water temperature.

Fig. 16 shows the effect of water temperature on the degradation of epoxy coatings after water impingement test for 90 min using tap water at a nozzle distance of 10 mm and water velocity of 139 m/s. At the water temperature of 15 °C, the difference of degradation rate was relatively small, but increasing the water temperature greatly increased the difference. Fig. 16d shows the effect of water temperature on the rate after 90 min test, and among the three epoxy coatings, C coating showed higher resistance to the effect of water temperature. In particular, the degradation rate of C coating was almost constant in the test temperature range.

Fig. 17 shows the effect of water temperature on SEM images (center area) after water impingement test for 90 min using tap water at a nozzle distance of 10 mm and water velocity of 139 m/s. In the case of A and B coatings, a deep cavity by water impingement was formed. However, in the case of C coating, some pores emerged, but there was little damage in the range of test temperature. Fig. 18 shows the effect of water temperature on Si strengthener by EDS (center area) after water impingement test for 90 min using tap water at a nozzle distance of 10 mm and water velocity of 139 m/s. In the case of A and B coatings, the glass flakes were detached,

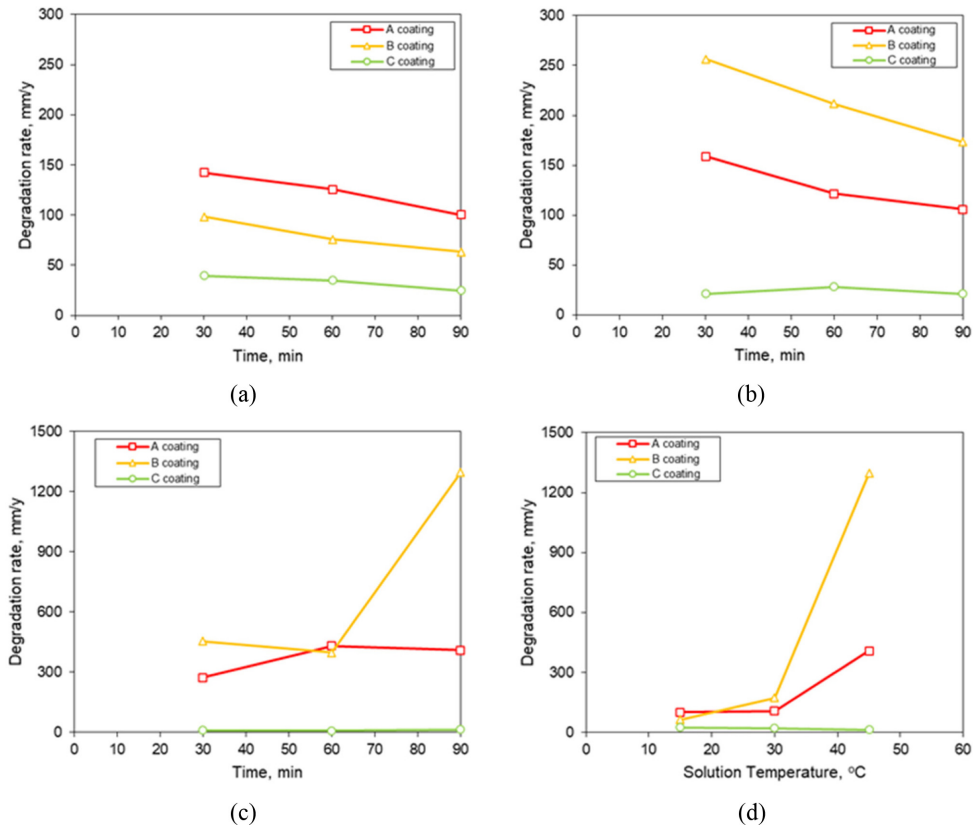

Fig. 16. Effect of water temperature on the degradation of epoxy coatings after water impingement test for 90 min using tap water at a nozzle distance of 10 mm and water velocity of 139 m/s: (a) 15 °C, (b) 30 °C, (c) 45 °C, and (d) degradation rate after test

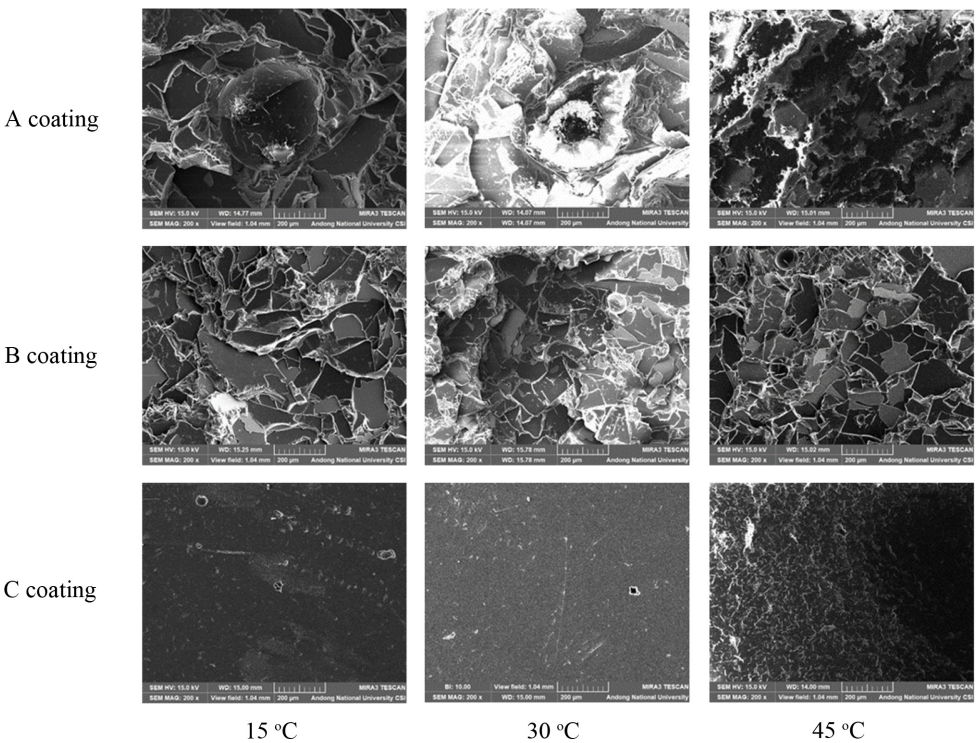

Fig. 17. Effect of water temperature on SEM images (center area) after water impingement test for 90 min using tap water at a nozzle distance of 10 mm and water velocity of 139 m/s

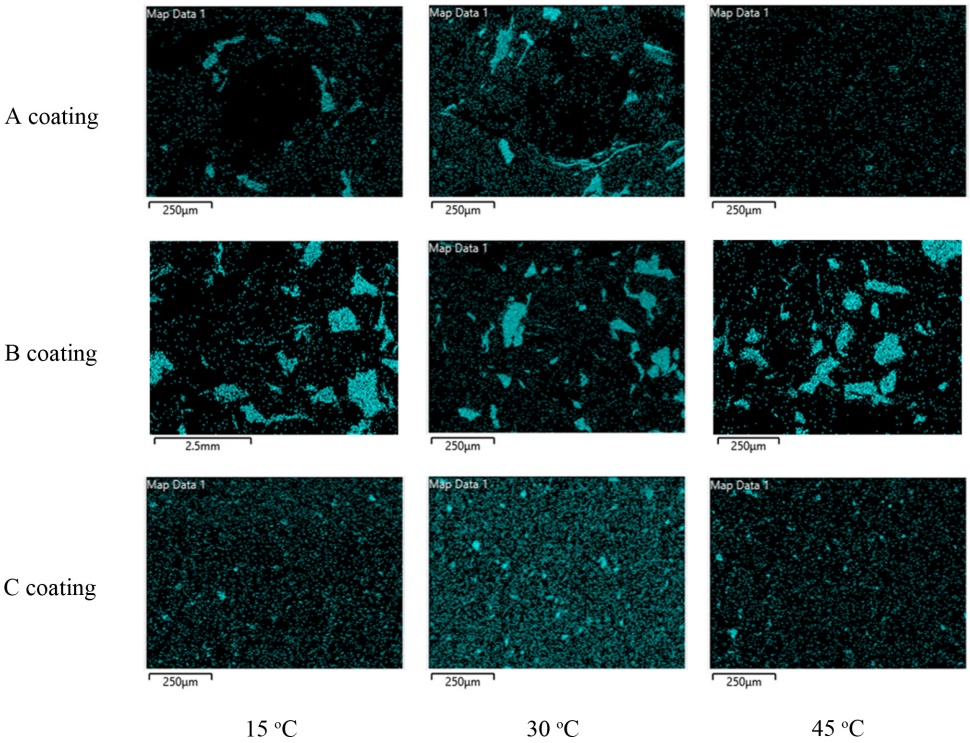

Fig. 18. Effect of water temperature on Si strengthener by EDS (center area) after water impingement test for 90 min using tap water at a nozzle distance of 10 mm and water velocity of 139 m/s

and the Si distribution was non-uniform. However, in the case of C coating, the Si distribution was similar to that of the specimen before test, as shown in Fig. 2.

In summary, in the case of A and B coatings, the surface appearance was severely degraded, and the glass flake did not reveal good performance as a strengthening component in the water impingement test. However, in the case of C coating, ceramic compound in the epoxy resin showed the best performance, as discussed in the cavitation test [19,20]. We have reported that their resistance was closely related the flexural strength, tensile strength, wear resistance, and pull-off strength of the coating [19,20]. In addition to the mechanical properties of the coating, small and polygonal compounds were also effective for the cavitation resistance of C coating [19,20]. Based on the observations described above, the water impingement mechanism of epoxy coatings was proposed. Figure 19 shows the degradation steps of epoxy coatings by water impingement test in tap water. Step 1 is the epoxy resin failure stage. Step 2 is the strengthening component failure stage, and in this stage, the compound or the matrix or the interface of the matrix and compound, depending upon the components used in the coatings, were partly damaged.

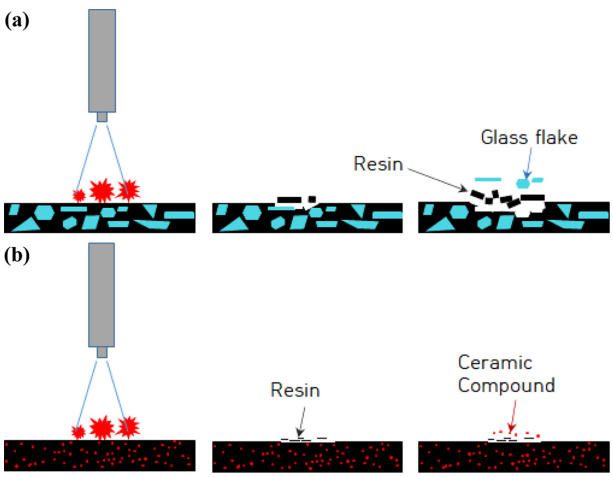

Fig. 19. Schematic of the failure mechanism of epoxy coatings by water impingement test: (a) A and B coatings, and (b) C coating

4. Conclusions

In this work, three kinds of epoxy coatings from three different companies were used, and the water impingement properties of the coatings were evaluated in tap water

at different temperatures, controlling the water velocity and nozzle distance. We found that:

Increasing water velocity and water temperature and reducing nozzle distance increased the degradation rates of the three epoxy coatings. This behavior is related to small and polygonal compounds being effective for the water impingement resistance of epoxy coatings, in addition to the mechanical properties of the coating.

The increase in degradation rate of A and B coatings by increasing water velocity was higher than that of C coating; the increase in degradation rate of A and B coatings by reducing nozzle distance was faster than that of C coating; the increase in degradation rate of A and B coatings by increasing water temperature was greater than that of C coating. Among the three test parameters, water temperature was relatively effective to increase the degradation rate of epoxy coatings.

Acknowledgments

This work was supported by KOREA HYDRO & NUCLEAR POWER CO., LTD (No. 2019-Technical-08). This research was also partly supported by Korea Institute for Advancement of Technology (KIAT) grant funded by the Korea Government (MOTIE) (P0008458, HRD Program for Industrial Innovation, 2022).

References

1. S. Nesic, Key issues related to modelling of internal corrosion of oil and gas pipelines – A review, *Corrosion Science*, **49**, 4308 (2007). Doi: https://doi.org/10.1016/j.corsci.2007.06.006
2. J. A. Jeong, M. S. Kim, S. D. Yang, C. H. Hong, N. K. Lee, and D. H. Lee, Study of the electrochemical polarization test of carbon steel in natural seawater, *Journal of the Korean Society of Marine Engineering*, **42**, 274 (2018). Doi: https://doi.org/10.5916/jkosme.2018.42.4.274
3. A. A. B. Saleh, K. K. Dinesh, R. ElanseZhian, Development of Corrosion Resistance Coatings for Sea Water Pipeline, *International Journal of Students' Research in Technology & Management*, **4**, 24 (2016). Doi: https://doi.org/10.18510/ijsrtm.2016.421
4. Y. Huang, D. Ji, Experimental study on seawater-pipeline internal corrosion monitoring system, *Sensors and Actuators B: Chemical*, **135**, 375 (2008). Doi: https://doi.org/10.1016/j.snb.2008.09.008
5. S. Y. Lee, K. H. Lee, C. U. Won, S. Na, Y. G. Yoon, M. H. Lee, Y. H. Kim, K. M. Moon, J. G. Kim, Electrochemical Evaluation of Corrosion Property of Welded Zone of Seawater Pipe by DC Shielded Metal Arc Welding with Types of Electrodes, *Ocean Engineering and Technology,* **27**, 79 (2013). Doi: https://doi.org/10.5574/KSOE2013.27.3.079
6. F. W. Fink, Saline water conversion*,* American Chemical Society: Washington DC, **1**, 27 (1960). Doi: https://doi.org/10.1021/ba-1963-0038.fw001
7. S. J. Kim, Apparatus on Corrosion Protection and Marine Corrosion of Ship, *The Korean Institute of Surface Engineering*, **44**, 105 (2011). Doi: https://doi.org/10.5695/JKISE.2011.44.3.105
8. J. A. Jeong, M. S. Kim, S. D. Yang, C. H. Hong, N. K. Lee, D. H. Lee, Cathodic protection using insoluble anodes by delivering protection currents to the inner surfaces of carbon steel seawater pipes, *Journal of the Korean Society of Marine Engineering*, **42**, 280 (2018). Doi: https://doi.org/10.5916/jkosme.2018.42.4.280
9. C. Chandrasekaran, Anticorrosive rubber lining*, Elsevier Science*, **1**, 43 (2017). Doi: https://doi.org/10.1016/B978-0-323-44371-5.00006-2
10. J. W. Kim, Protection Technique by coating and lining. *Journal of the Korean Society of Marine Engineers*, **24***,* 539 (2000). Doi: https://koreascience.kr/article/JAKO200011919930815.page
11. M. S. Camila, S. Deborah, S. G. Thiago, Coatings for saltwater pipelines, *International Journal of Advanced Engineering Research and Science,* **5**, 266 (2018). Doi: https://doi.org/10.26678/ABCM.CONEM2018.CON18-1168
12. I. Tzanakis, L. Bolzoni, D. G. Eskin, and M. Hadfield, Evaluation of cavitation erosion behavior of commercial steel grades used in the design of fluid machinery, *Metallurgical and Materials Transaction A*, **48A**, 2193 (2017). Doi: https://doi.org/10.1007/s11661-017-4004-2
13. H. Sun, Numerical study of hydrofoil geometry effect on cavitating flow, *Journal of Mechanical Science and Technology*, **26**, 8, 2535(2012) Doi: https://doi.org/10.1007/s12206-012-0633-y
14. F. Galliano, D. Landolt, Evaluation of corrosion protection properties of additives for waterborne epoxy coatings on steel, *Progress in Organic Coatings*, **44**, 217 (2002). Doi: https://doi.org/10.1016/S0300-9440(02)00016-4
15. A. Talo, O. Forsén, S. Yläsaari, Corrosion protective polyaniline epoxy blend coatings on mild steel, *Synthetic*

Metals, **102**, 1394 (1999). Doi: https://doi.org/10.1016/S0379-6779(98)01050-9

16. V.B. Miskovic-Stankovic, M.R. Stanic, D.M. Drazic, Corrosion protection of aluminium by a cataphoretic epoxy coating, *Progress in Organic Coatings*, **36**, 53 (1999). Doi: https://doi.org/10.1016/S0300-9440(99)00024-7
17. I. J. Jang, K. T. Kim, Y. R. Yoo, Y. S. Kim, Effects of Ultrasonic Amplitude on Electrochemical Properties During Cavitation of Carbon Steel in 3.5% NaCl Solution, *Corrosion Science and Technology*, **19**, 163 (2020). Doi: https://doi.org/10.14773/cst.2020.19.4.163
18. I. J. Jang, J. M. Jeon, K. T. Kim, Y. R. Yoo, Y. S. Kim, Ultrasonic Cavitation Behavior and its Degradation Mechanism of Epoxy Coatings in 3.5 % NaCl at 15 °C, *Corrosion Science and Technology*, **20**, 26 (2021). Doi: https://doi.org/10.14773/cst.2021.20.1.26
19. J. M. Jeon, Y. R. Yoo, Y. S. Kim, Effect of Solution Temperature on the Cavitation Corrosion Properties of Carbon Steel and its Electrochemical Effect, *Corrosion Science and Technology*, **20**, 325 (2021). Doi: https://doi.org/10.14773/cst.2021.20.6.325
20. J. M. Jeon, Y. R. Yoo, M. J. Jeong, Y. C. Kim, Y. S. Kim, Effect of Solution Temperature on the Cavitation Degradation Properties of Epoxy Coatings for Seawater Piping, *Corrosion Science and Technology*, **20**, 335 (2021). Doi: https://doi.org/10.14773/cst.2021.20.6.335
21. I. C. Park, M. S. Han, S. J. Kim, Optimization of Painting Process to Improve Durability of Mega Yacht and Cavitation Erosion Characteristics, *Welding and Joining*, **37**, 254 (2019). Doi: https://doi.org/10.5781/JWJ.2019.37.3.9
22. J. H. Lee, J. H. Kim, Y. P. Kim, S. J. Kim, Evaluation of Anti-Cavitation Performance of Polyurethane Coatings in Seawater using Ultrasonic Vibratory Method, *Welding and Joining*, **37**, 455 (2019). Doi: https://doi.org/10.5781/JWJ.2019.37.5.4
23. S. Hattori, T. Itoh, Cavitation erosion resistance of plastics, *Wear*, **271**, 1103 (2011). Doi: https://doi:10.1016/j.wear.2011.05.012
24. S. J. Kim, S. O. Chong, Characteristics of surface damage with applied current density and cavitation time variables for 431 stainless steel in seawater, *Journal of the Korean Society of Marine Engineering*, **38**, 883 (2014). Doi: https://doi.org/10.5916/jkosme.2014.38.7.883
25. F. T. Cheng, P. Shi, H. C. Man, Correlation of cavitation erosion resistance with indentation-derived properties for a NiTi alloy, *Script Materialia*, **45**, 1083 (2001). Doi: https://doi.org/10.1016/S1359-6462(01)01143-5
26. M. Rein, Phenomena of liquid drop impact on solid and liquid surfaces, *Fluid Dynamics Research*, **12**, 61 (1993). Doi: https://doi.org/10.1016/0169-5983(93)90106-K
27. K. S. Park, Y. K. Bahk, J. S. Go, B. S. Shin, A Study on the Frosting Phenomena of Abrasive Waterjet Micro cutting for Multi-Layered Materials, *Transactions of the Korean Society of Machine Tool Engineers*, **16**, 183 (2007). Doi: https://koreascience.kr/article/JAKO200734516353892.page
28. J. Bhandari, F. Khan, R. Abbassi, V. Garaniya, and R. Ojeda, Modelling of pitting corrosion in marine and offshore steel structures e A technical review, *Journal of Loss Prevention in the Process Industries*, **37**, 39 (2015). Doi: https://doi.org/10.1016/j.jlp.2015.06.008
29. ISO 16925, Paints and varnishes — Determination of the resistance of coatings to pressure water-jetting (2014).
30. Y. S. Kim, Report on the Evaluation of Lining Materials for the Inside Coating of Seawater Piping of Kori #3 and #4 Nuclear Power Plants, Final Report, p. 157, KEPCO E&C, Feb. (2020).